

Coevolution of superconductivity and Hall coefficient with anisotropic lattice shrinkage in compressed $KCa_2Fe_4As_4F_2$

Jinyu Han(韩金宇), Wenshan Hong(洪文山), Shu Cai(蔡树), Jinyu Zhao(赵金瑜), Jing Guo(郭静), Yazhou Zhou(周亚洲), Pengyu Wang(王鹏玉), Lixin Cao(曹立新), Huiqian Luo(罗会仟), Shiliang Li(李世亮), Qi Wu(吴奇), and Liling Sun(孙力玲)

Citation: Chin. Phys. B, 2024, 33 (**7**): 077402. DOI: 10.1088/1674-1056/ad4d65
Journal homepage: http://cpb.iphy.ac.cn; http://iopscience.iop.org/cpb

What follows is a list of articles you may be interested in

Co-doped $BaFe_2As_2$ Josephson junction fabricated with a focused helium ion beam

Ziwen Chen(陈紫雯), Yan Zhang(张焱), Ping Ma(马平), Zhongtang Xu(徐中堂), Yulong Li(李宇龙), Yue Wang(王越), Jianming Lu(路建明), Yanwei Ma(马衍伟), and Zizhao Gan(甘子钊)

Chin. Phys. B, 2024, 33 (**4**): 047405. DOI: 10.1088/1674-1056/ad21f7

Majorana tunneling in a one-dimensional wire with non-Hermitian double quantum dots

Peng-Bin Niu(牛鹏斌) and Hong-Gang Luo(罗洪刚)

Chin. Phys. B, 2024, 33 (**1**): 017403. DOI: 10.1088/1674-1056/ad0145

Advances in thermoelectric $(GeTe)_x(AgSbTe_2)_{100-x}$

Hongxia Liu(刘虹霞), Xinyue Zhang(张馨月), Wen Li(李文), and Yanzhong Pei(裴艳中)

Chin. Phys. B, 2022, 31 (**4**): 047401. DOI: 10.1088/1674-1056/ac3cae

Effects of pressure and/or magnetism on superconductivity of δ-MoN single crystal

Miao Bo-Tong (苗博童), Wang Shan-Min (王善民), Kong Pan-Pan (孔盼盼), Jin Mei-Ling (金美玲), Feng Shao-Min (冯少敏), Zhang Si-Jia (张思佳), Hao Ai-Min (郝爱民), Yu Xiao-Hui (于晓辉), Jin Chang-Qing (靳常青), Zhao Yu-Sheng (赵予生)

Chin. Phys. B, 2015, 24 (**1**): 017403. DOI: 10.1088/1674-1056/24/1/017403

Crystal chemistry and structural design of iron-based superconductors

Jiang Hao (蒋好), Sun Yun-Lei (孙云蕾), Xu Zhu-An (许祝安), Cao Guang-Han (曹光旱)

Chin. Phys. B, 2013, 22 (**8**): 087410. DOI: 10.1088/1674-1056/22/8/087410

RAPID COMMUNICATION

Coevolution of superconductivity and Hall coefficient with anisotropic lattice shrinkage in compressed $KCa_2Fe_4As_4F_2$

Jinyu Han(韩金宇)[1,3], Wenshan Hong(洪文山)[1], Shu Cai(蔡树)[2], Jinyu Zhao(赵金瑜)[1,3], Jing Guo(郭静)[1], Yazhou Zhou(周亚洲)[1], Pengyu Wang(王鹏玉)[1,3], Lixin Cao(曹立新)[1], Huiqian Luo(罗会仟)[1,3], Shiliang Li(李世亮)[1,3], Qi Wu(吴奇)[1], and Liling Sun(孙力玲)[1,2,3,†]

[1] *Beijing National Laboratory for Condensed Matter Physics, Institute of Physics, Chinese Academy of Sciences, Beijing* 100190, *China*
[2] *Center for High Pressure Science & Technology Advanced Research, Beijing* 100094, *China*
[3] *University of Chinese Academy of Sciences, Beijing* 100190, *China*

(Received 2 May 2024; revised manuscript received 16 May 2024; accepted manuscript online 20 May 2024)

The stability of superconductivity in superconductors is widely recognized to be determined by various factors, including charge, spin, orbit, lattice, and other related degrees of freedom. Here, we report our findings on the pressure-induced coevolution of superconductivity and Hall coefficient in $KCa_2Fe_4As_4F_2$, an iron-based superconductor possessing a hybrid crystal structure combining KFe_2As_2 and CaFeAsF. Our investigation, involving high-pressure resistance, Hall effect and x-ray diffraction (XRD) measurements, allows us to observe the connection of the superconductivity and Hall coefficient with the anisotropic lattice shrinkage. We find that its ambient-pressure tetragonal (T) phase presents a collapse starting at around 18 GPa, where the sign of the Hall coefficient (R_H) changes from positive to negative. Upon further compression, both superconducting transition temperature (T_c) and R_H exhibit a monotonous decrease. At around 41 GPa, the superconductivity is completely suppressed ($T_c = 0$), where the parameter a begins to decline again and the Hall coefficient remains nearly unchanged. Our experiment results clearly demonstrate that the pressure-induced anisotropic lattice collapse plays a crucial role in tuning the interplay among multiple degrees of freedom in the superconducting system and, correspondingly, the stability of the superconductivity.

Keywords: effects of pressure, pnictides and chalcogenides, transport properties

PACS: 74.62.Fj, 74.70.Xa, 74.25.F– **DOI:** 10.1088/1674-1056/ad4d65

The discovery of iron-based superconductors[1,2] provides a new opportunity for better understanding the mechanism of high-T_c superconductivity, a topic that has been the subject of debate for over three decades. Currently, various types of iron-pnictide superconductors with different structures have been identified. These types primarily include superconductors with stacking sequences of LaOFeAs (1111), Sr_2VO_3FeAs (21311), FeSe (11), $BaFe_2As_2$ (122), $CaKFe_4As_4$ (1144), and $KCa_2Fe_4As_4F_2$ (12442).[1,3–7] Among this kind of superconductors, there exists a distinct group that displays unique characteristics. Examples of such superconductors include $Ca_{10}(Pt_4As_8)(Fe_2As_2)_5$ (1048),[8] $Ba_2Ti_2Fe_2As_4O$ (22241),[9] 1144,[6] and 12442[7,10] superconductors, which have specific chemical compositions with stoichiometry. This allows them to exhibit intrinsic superconductivity without the requirement of chemical doping. The findings of these stoichiometric superconductors provide a remarkable platform for understanding the mechanism of the high-T_c superconductivity because they significantly reduce the complexity associated with the inhomogeneous local structure from chemical doping.

There is consensus that the stability of superconductivity of iron-based superconductors is highly related to the Fe–As coupling.[11,12] Notably, high pressure has proven to be an effective method for manipulating superconductivity and electronic structure.[13–24] In particular, the application of high pressure allows for the adjustment of the bond length within the Fe–As layer through lattice compression.[25] Recent high-pressure studies on the stoichiometric 1144 superconductors found that the transition from a half-collapse to a full-collapse of the tetragonal phase has a profound impact on the superconductivity[25–28] due to the reconstruction of Fermi surface.[25] In comparison to the 1144 superconductor, the 12442 superconductor possesses a more complex crystal structure.[7,29–31] It can be viewed as an intergrowth structure that combines the alternating layers of KFe_2As_2 and CaFeAsF.[7,10] This structure includes double Fe_2As_2 layers with K atoms sandwiched in between, and these layers are separated by a Ca_2F_2 layer. Consequently, the 12442 superconductor exhibits two different sites for As ions within the tetragonal unit cell, namely, As(1) and As(2), with a space group $I4/mmm$.[7,10] Upon cooling, $KCa_2Fe_4As_4F_2$ exhibits superconductivity with a critical temperature (T_c) around 33 K. Notably, angle-resolved photoemission spectroscopy and specific heat experiments have revealed that this material possesses a complex electronic

†Corresponding author. E-mail: llsun@iphy.ac.cn; liling.sun@hpstar.ac.cn

© 2024 Chinese Physical Society and IOP Publishing Ltd

structure and multigap properties,[29,32–34] consistent with the theoretical calculations.[35] However, the gap symmetry of $KCa_2Fe_4As_4F_2$ remains a subject of controversy.[32–34,36,37] Previous high-pressure studies conducted on the 12442 superconductor up to 15 GPa have demonstrated that the superconducting transition temperature (T_c) initially increases, reaches a maximum of $T_c = 36.5$ K at 2 GPa and then decreases upon further compression, and no iso-structural phase transition was observed within the investigated pressure range.[38] Given that the 12442 superconductor shares a similar structure to that of the 1144 superconductor, which demonstrates a close relationship between T_c, Hall coefficient, and lattice structure under pressure, it becomes highly intriguing to investigate whether the 12442 superconductor also exhibits the same correlation under higher pressure. This investigation aims to assess how the lattice shrinkage impacts the Fe–As coupling in stabilizing superconductivity in a different material.

High-quality single crystals of $KCa_2Fe_4As_4F_2$ were grown using the self-flux method, as reported previously.[7,39] The superconducting critical temperature at ambient pressure was confirmed to be 33.5 K, in good agreement with the results reported before.[7,10] High pressure was generated by a diamond anvil cell made of BeCu alloy with two opposing anvils. Diamond anvils with 300 μm culet (flat area of the diamond anvil) were employed for several independent measurements. In the high-pressure resistance and Hall measurements, the Van der Pauw method was used, following the technique described by Van der Pauw in Philips.[40] Platinum foil was used as the electrodes, a rhenium plate as the gasket, cubic boron nitride as the insulating material, and NaCl as the pressure medium. High-pressure x-ray diffraction (XRD) measurements were carried out at beamline 15U of the Shanghai Synchrotron Radiation Facility. A monochromatic x-ray beam with a wavelength of 0.6199 Å was employed for these measurements. The pressure for all measurements was determined using the ruby fluorescence method.[41]

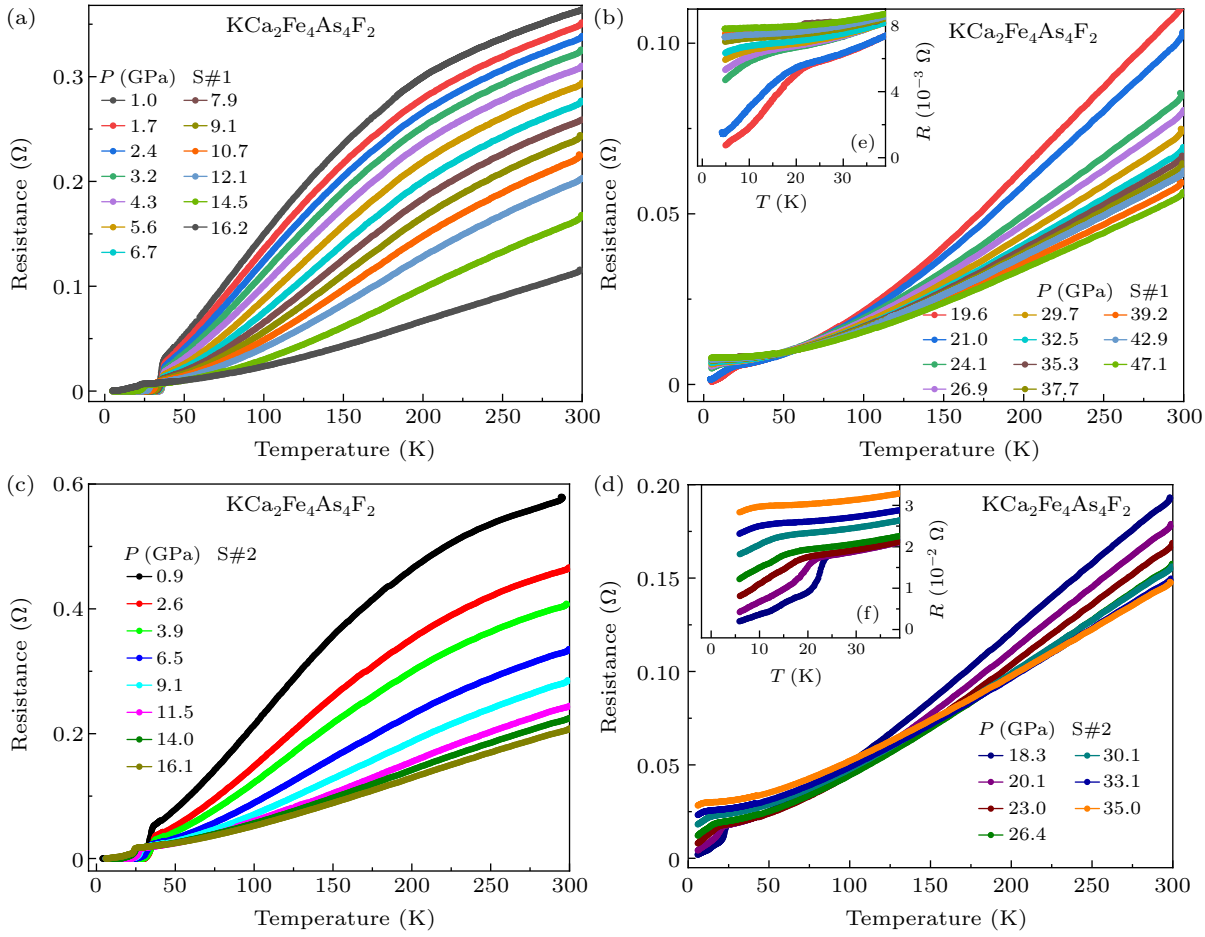


Fig. 1. Temperature dependence of resistance for the two $KCa_2Fe_4A_2$ samples under pressures ranging from 1.0 GPa–16.2 GPa (a) and 19.6 GPa–47.1 GPa (b) for S#1, 0.9 GPa–16.1 GPa (c) and 18.3 GPa–35.0 GPa (d) for S#2. The insets of panels (b) and (d) display low temperature resistances of the two samples.

First, we performed *in-situ* resistance measurements on the $KCa_2Fe_4As_4F_2$ samples in a diamond anvil cell. Figure 1 illustrates the variation in electrical resistance as a function of temperature for two samples (S#1 and S#2) at different pressures up to 47.1 GPa and 35.0 GPa, respectively. It is seen that the superconducting critical temperatures (T_c) of both samples increase initially. For S#1, T_c reaches a maximum of 37.5 K at around 2.4 GPa (Fig. 1(a)). Similarly, for S#2, T_c increases

to 37.3 K at around 2.6 GPa (Fig. 1(c)). These observations align with the results reported in a previous study.[38] Upon further increasing the pressure, T_c exhibits a monotonic decrease (Figs. 1(b) and 1(d)) and is completely suppressed at pressure between 39.2 GPa and 42.9 GPa (Fig. 1(b)). Here we take the average value ($[39.2+42.9]/2 = 41.05$ GPa) as the critical pressure for the transition from superconducting to non-superconducting state.

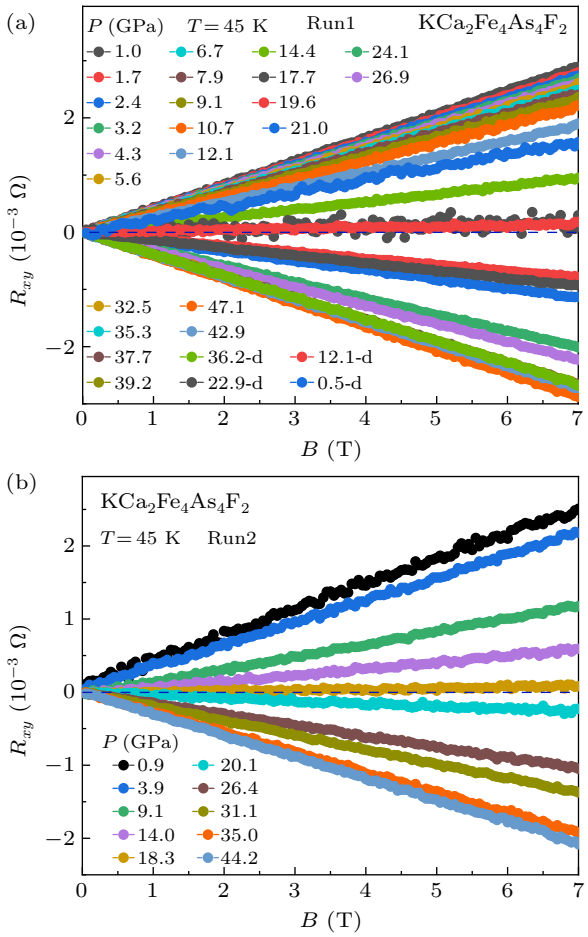


Fig. 2. Hall resistance (R_{xy}) as a function of magnetic field (B) for the two $KCa_2Fe_4As_4F_2$ samples at different pressures. In (a), the data labeled by 36.2-d, 22.9-d, 12.1-d and 0.5-d are the results obtained from the releasing pressure measurements.

To understand the pressure-induced change in T_c with normal state transport properties for the 12442 superconductor, high-pressure Hall resistance (R_{xy}) measurements were performed on the samples S#1 and S#2 through sweeping the magnetic field (B) applied perpendicular to the *ab* plane of those two samples from 0 T to 7 T at 45 K, as shown in Fig. 2. We found that the plot of R_{xy} versus B exhibits positive relationship below 17.7 GPa for S#1 and 18.3 GPa for S#2, indicating that hole carriers are dominated within the pressure range. However, $R_{xy}(B)$ changes its sign from positive to negative at about 17.7 GPa for S#1 and 18.3 GPa for S#2, revealing that the dominant carriers in this superconductor change from the hole-type into the electron-type.

To ensure a reasonable estimation, we consider the average value obtained from the two independent runs of measurements on the samples as the critical pressure ($P_c = [17.7+18.3]/2 = 18$ GPa). Based on these results, we propose that a significant Fermi surface reconstruction from a hole dominated to an electron dominated one occurs at about 18 GPa.

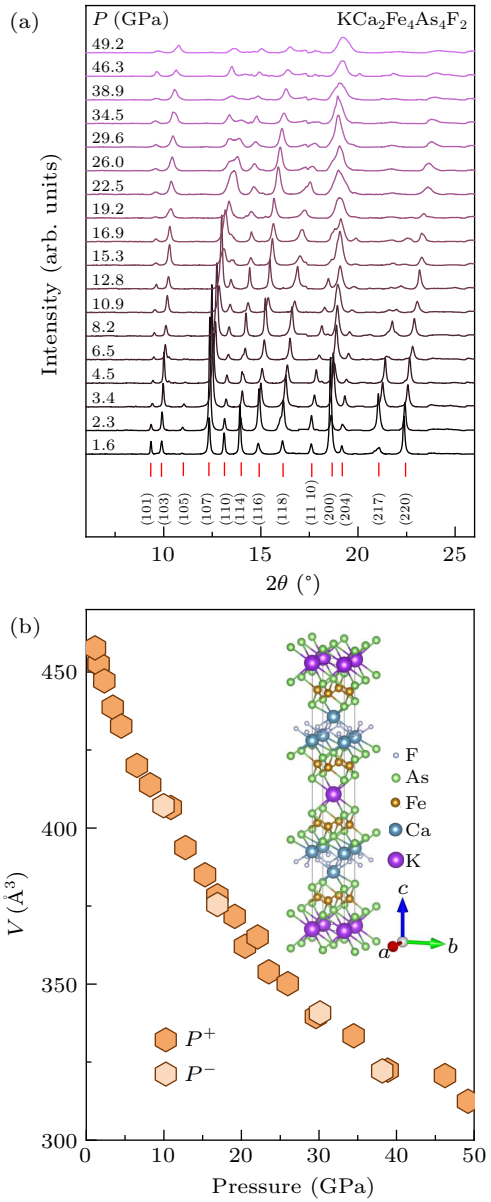


Fig. 3. XRD results of the $KCa_2Fe_4As_4F_2$ sample under different pressures. (a) XRD patterns collected at different pressures, showing no first-order structural phase transition up to 49.2 GPa. (b) The pressure dependence of volume (V). The inset illustrates the unique crystal structure of the 12442 superconductor.

Since the superconductivity usually has an intimate connection with the lattice structure, we conducted x-ray diffraction (XRD) measurements on the 12442 sample under pressures up to 49.2 GPa, with an aim to know how the changes in superconductivity and Hall resistance are accompanied by lattice shrinkage. Figure 3(a) displays the XRD results obtained from the 12442 sample at different pressures. We found that all

the observed peaks can be indexed well by the tetragonal (T) phase in the $P4/mmm$ space group. Based on these results, we extracted the pressure dependence of lattice parameters (they will be discussed later) and volume (Fig. 3(b)). The gradual decrease in volume signifies the absence of any first-order phase transition within the pressure range up to 49.2 GPa.

We summarize our high-pressure experimental results obtained from the measurements on the 12442 superconductors in the pressure–T phase diagram (Fig. 4(a)). The diagram reveals three distinct regimes. In the low-pressure regime (below P_{c1}), the sample maintains its T phase, wherein the superconducting temperature T_c displays an increase initially from 33.5 K to 36.5 K at 2.4 GPa, followed by a steady decrease (Fig. 4(a)). Within this regime, we observed a reduction in both lattice parameters a and c (Fig. 4(b)) and the hole-type carriers are dominating (Fig. 4(c)).

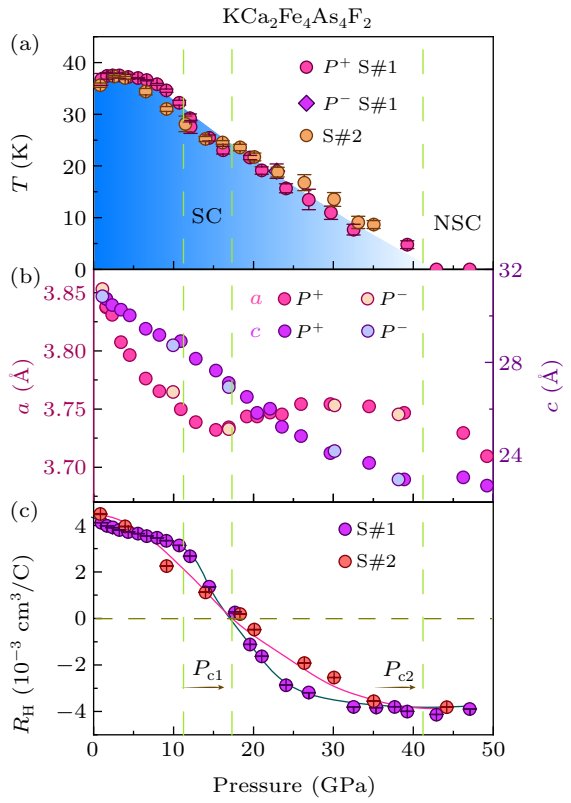


Fig. 4. Coevolution of superconductivity, crystal structure and Hall coefficient of $KCa_2Fe_4As_4F_2$ under pressures. (a) Pressure–temperature phase transition, revealing a pressure-induced change in T_c. (b) Pressure dependence of lattice parameters a and c, illustrating a pressure-induced half collapsed tetragonal phase starting at P_{c1} ($\sim$ 18 GPa) and full collapsed tetragonal phase at P_{c2} ($\sim$ 41 GPa). (c) Pressure dependence of Hall coefficient, showing the pressure-induced change from the hole-type carrier to the electron-type one at P_{c1}, and remaining unchanged at pressure above P_{c2}.

Intriguingly, at P_{c1}, we observe a notable expansion in the lattice parameter a (Fig. 4(b)). This phenomenon is reminiscent of what has been observed in the 1144 superconductors, where the lattice parameter a also undergoes a sudden increase while the volume continues to decrease. These observations suggest that the 12442 superconductor also undergoes an iso-structure transition from the tetragonal (T) phase to the collapsed tetragonal (cT) phase at P_{c1}. Interestingly, at this critical pressure, the Hall coefficient (R_H) undergoes a sign change from positive to negative, like what has been observed in the 1144 superconductors.[25–27,42–44] As the pressure is increased, we observe a gradual increase in the lattice parameter a (Fig. 4(b)), accompanied by a continued decrease in T_c (Fig. 4(a)). At P_{c2}, the sample loses its superconductivity ($T_c = 0$, see Fig. 4(a)), and the lattice parameter a begins to decline again (Fig. 4(b)), suggesting that pressure-induced collapse of the T phase is completed. This observation generally aligns with the behavior observed in the 1144 superconductor,[25,42,43] however the superconductivity in the latter is entirely suppressed upon a full collapse of the T phase. Upon further increasing the pressure beyond P_{c2}, we find that the lattice parameter a starts to decrease and R_H remains nearly unchanged (Fig. 4(c)).

Previous calculations have suggested that Fe–As coupling plays a pivotal role in developing or stabilizing superconductivity of iron pnictides.[11] Considering the unique structure of the 12442 superconductor, the pressure-induced transitions of the cT phase appear to promote the formation of the As–As bonding across the K layer, similar to what has been observed in the 1144 superconductors.[11,25,27,42] These bond formations inevitably weaken the Fe–As coupling, which significantly impacts the electronic structure and, consequently, the superconductivity. This experimental observation provides further evidence of the crucial role played by Fe–As coupling in stabilizing the superconductivity of iron pnictides. In addition, our results show that the pressure-induced coevolution of superconductivity and Hall coefficient with the lattice shrinkage is reversible, as presented in Figs. 3 and 4, which deserves further investigations.

In conclusion, we report the coevolution of superconductivity and Hall coefficient, along with the anisotropic lattice shrinkage, in compressed $KCa_2Fe_4As_4F_2$ up to 47.1 GPa. Our results clearly demonstrate that below the first critical pressure ($P_{c1} = 18$ GPa), superconducting transition temperature (T_c) displays an increase initially and then exhibits a monotonous decrease. Hall measurements find that the hole-type carriers are dominating in this pressure range. At around P_{c1}, we observed that the sample undergoes an iso-structure phase transition from its initial tetragonal (T) phase to a collapsed T (cT) phase, concurrently, the Hall coefficient undergoes a sign change from positive to negative. Upon increasing the pressure above P_{c1}, the superconducting transition temperature (T_c) exhibits a continuous decrease. At the second critical pressure ($P_{c2} = 41$ GPa), the sample completely loses its superconductivity, associated with the complete collapse of the T phase, while the Hall coefficient remains nearly unchanged. These results demonstrate that the pressure-induced anisotropic lattice collapse plays a crucial role in tuning the

interplay among the multiple degrees of freedom in the superconducting system and, correspondingly, the stability of the superconductivity.

Acknowledgments

Project supported by the National Key Research and Development Program of China (Grant Nos. 2022YFA1403900, 2021YFA1401800, 2018YFA0704201, and 2023YFA1406103), the National Natural Science Foundation of China (Grant Nos. U2032214, 12122414, 12104487, and 12004419), and the Strategic Priority Research Program (B) of the Chinese Academy of Sciences (Grant No. XDB25000000).

References

[1] Kamihara Y, Watanabe T, Hirano M and Hosono H 2008 *J. Am. Chem. Soc.* **130** 3296
[2] Ren Z A, Lu W, Yang J, Yi W, Shen X L, Li Z C, Che G C, Dong X L, Sun L L, Zhou F and Zhao Z X 2008 *Chin. Phys. Lett.* **25** 2215
[3] Zhu X, Han F, Mu G, Cheng P, Shen B, Zeng B and Wen H H 2009 *Phys. Rev. B* **79** 220512
[4] Hsu F C, Luo J Y, Yeh K W, Chen T K, Huang T W, Wu P M, Lee Y C, Huang Y L, Chu Y Y, Yan D C and Wu M K 2008 *Proc. Natl. Acad. Sci. USA* **105** 14262
[5] Rotter M, Tegel M and Johrendt D 2008 *Phys. Rev. Lett.* **101** 107006
[6] Iyo A, Kawashima K, Kinjo T, Nishio T, Ishida S, Fujihisa H, Gotoh Y, Kihou K, Eisaki H and Yoshida Y 2016 *J. Am. Chem. Soc.* **138** 3410
[7] Wang Z C, He C Y, Wu S Q, Tang Z T, Liu Y, Ablimit A, Feng C M and Cao G H 2016 *J. Am. Chem. Soc.* **138** 7856
[8] Ni N, Allred J M, Chan B C and Cava R J 2011 *Proc. Natl. Acad. Sci. USA* **108** E1019
[9] Sun Y L, Jiang H, Zhai H F, Bao J K, Jiao W H, Tao Q, Shen C Y, Zeng Y W, Xu Z A and Cao G H 2012 *J. Am. Chem. Soc.* **134** 12893
[10] Wang T, Chu J, Jin H, Feng J, Wang L, Song Y, Zhang C, Xu X, Li W, Li Z, Hu T, Jiang D, Peng W, Liu X and Mu G 2019 *J. Phys. Chem. C* **123** 13925
[11] Yang R, Le C, Zhang L, Xu B, Zhang W, Nadeem K, Xiao H, Hu J and Qiu X 2015 *Phys. Rev. B* **91** 224507
[12] Yang R, Dai Y, Xu B, Zhang W, Qiu Z, Sui Q, Homes C C and Qiu X 2017 *Phys. Rev. B* **95** 064506
[13] Struzhkin V V, Hemley R J, Mao H k and Timofeev Y A 1997 *Nature* **390** 382
[14] Shimizu K, Kimura T, Furomoto S, Takeda K, Kontani K, Onuki Y and Amaya K 2001 *Nature* **412** 316
[15] Mao W L, Mao H k, Eng P J, Trainor T P, Newville M, Kao C c, Heinz D L, Shu J, Meng Y and Hemley R J 2003 *Science* **302** 425
[16] Sun L, Chen X J, Guo J, Gao P, Huang Q Z, Wang H, Fang M, Chen X, Chen G, Wu Q, Zhang C, Gu D, Dong X, Wang L, Yang K, Li A, Dai X, Mao H K and Zhao Z 2012 *Nature* **483** 67
[17] Chen X J, Struzhkin V V, Yu Y, Goncharov A F, Lin C T, Mao H K and Hemley R J 2010 *Nature* **466** 950
[18] Deng L, Zheng Y, Wu Z, Huyan S, Wu H C, Nie Y, Cho K and Chu C W 2019 *Proc. Natl. Acad. Sci. USA* **116** 2004
[19] Guo J, Zhou Y, Huang C, Cai S, Sheng Y, Gu G, Yang C, Lin G, Yang K, Li A, Wu Q, Xiang T and Sun L 2019 *Nat. Phys.* **16** 295
[20] Zhou Y, Guo J, Cai S, Zhao J, Gu G, Lin C, Yan H, Huang C, Yang C, Long S, Gong Y, Li Y, Li X, Wu Q, Hu J, Zhou X, Xiang T and Sun L 2022 *Nat. Phys.* **18** 406
[21] Cai S, Zhao J, Ni N, Guo J, Yang R, Wang P, Han J, Long S, Zhou Y, Wu Q, Qiu X, Xiang T, Cava R J and Sun L 2023 *Nat. Commun.* **14** 3116
[22] Gao L, Xue Y Y, Chen F, Xiong Q, Meng R L, Ramirez D, Chu C W, Eggert J H and Mao H K 1994 *Phys. Rev. B* **50** 4260
[23] Huang Y E, Wu F, Wang A, Chen Y, Jiao L, Smidman M and Yuan H Q 2022 *Chin. Phys. Lett.* **39** 097101
[24] Jinyu Z, Shu C, Yiwen C, Genda G, Hongtao Y, Jing G, Jinyu H, Pengyu W, Yazhou Z, Yanchun L, Xiaodong L, Zhian R, Qi W, Xingjiang Z, Yang D, Tao X, Ho kwang M and Liling S 2024 *Chin. Phys. Lett.* **41** 047401
[25] Wang P, Liu C, Yang R, Cai S, Xie T, Guo J, Zhao J, Han J, Long S, Zhou Y, Li Y, Li X, Luo H, Li S, Wu Q, Qiu X, Xiang T and Sun L 2023 *Phys. Rev. B* **108** 054415
[26] Xiang L, Meier W R, Xu M, Kaluarachchi U S, Bud'ko S L and Canfield P C 2018 *Phys. Rev. B* **97** 174517
[27] Borisov V, Canfield P C and Valentí R 2018 *Phys. Rev. B* **98** 064104
[28] Xiang L, Xu M, Bud'ko S L and Canfield P C 2022 *Phys. Rev. B* **106** 134505
[29] Wu D, Hong W, Dong C, Wu X, Sui Q, Huang J, Gao Q, Li C, Song C, Luo H, Yin C, Xu Y, Luo X, Cai Y, Jia J, Wang Q, Huang Y, Liu G, Zhang S, Zhang F, Yang F, Wang Z, Peng Q, Xu Z, Qiu X, Li S, Luo H, Hu J, Zhao L and Zhou X J 2020 *Phys. Rev. B* **101** 224508
[30] Ishida J, Iimura S and Hosono H 2017 *Phys. Rev. B* **96** 174522
[31] Wang Z, He C, Tang Z, Wu S and Cao G 2016 *Science China Materials* **60** 83
[32] Duan W, Chen K, Hong W, Chen X, Yang H, Li S, Luo H and Wen H H 2021 *Phys. Rev. B* **103** 214518
[33] Hao J, Hong W, Zhou X, Xiang Y, Dai Y, Yang H, Li S, Luo H and Wen H H. 2022 *Phys. Rev. B* **106** 014523
[34] Li Y, Zhu Z, Ye Y, Hong W, Li Y, Li S, Luo H and Wen H H. 2024 *Phys. Rev. B* **109** 014506
[35] Wang G, Wang Z and Shi X 2016 *Europhys. Lett.* **116** 37003
[36] Kirschner F K K, Adroja D T, Wang Z C, Lang F, Smidman M, Baker P J, Cao G H and Blundell S J 2018 *Phys. Rev. B* **97** 060506
[37] Zhang C, Wu Q Y, Hong W S, Liu H, Zhu S X, Song J J, Zhao Y Z, Wu F Y, Liu Z T, Liu S Y, Yuan Y H, Huang H, He J, Li S, Liu H Y, Duan Y X, Luo H Q and Meng J Q 2022 *Sci. China Phys. Mech. Astron.* **65** 237411
[38] Wang B, Wang Z C, Ishigaki K, Matsubayashi K, Eto T, Sun J, Cheng J G, Cao G H and Uwatoko Y 2019 *Phys. Rev. B* **99** 014501
[39] Hong W, Song L, Liu B, Li Z, Zeng Z, Li Y, Wu D, Sui Q, Xie T, Danilkin S, Ghosh H, Ghosh A, Hu J, Zhao L, Zhou X, Qiu X, Li S and Luo H 2020 *Phys. Rev. Lett.* **125** 117002
[40] Pauw V D 1958 *Philips Research Reports* **13** 1
[41] Mao H K, Xu J and Bell P M 1986 *Journal of Geophysical Research: Solid Earth* **91** 4673
[42] Kaluarachchi U S, Taufour V, Sapkota A, Borisov V, Kong T, Meier W R, Kothapalli K, Ueland B G, Kreyssig A, Valentí R, McQueeney R J, Goldman A I, Bud'ko S L and Canfield P C 2017 *Phys. Rev. B* **96** 140501
[43] Stillwell R L, Wang X, Wang L, Campbell D J, Paglione J, Weir S T, Vohra Y K and Jeffries J R 2019 *Phys. Rev. B* **100** 045152
[44] Bud'ko S L, Kogan V G, Prozorov R, Meier W R, Xu M and Canfield P C 2018 *Phys. Rev. B* **98** 144520